Proceedings of the 25th International Conference on
Port and Ocean Engineering under Arctic Conditions
June 9-13, 2019, Delft, The Netherlands

Characterization of high pressure zone (*hpz*) failure and linkages with structural response during medium-scale indentation tests

Ridwan B. Hossain[1], Rocky S. Taylor[1]
Memorial University, St. John's, NL, Canada

ABSTRACT

The formation of high pressure zones (*hpz*s) during compressive ice failure results from a complex mixture of fracture and damage processes that lead to crushing and extrusion. The development of an *hpz* based dynamic ice-structure interaction model requires detailed understanding of these processes, as well modelling of the influence of structural response. In this paper, results from a recent series of medium-scale indentation tests conducted using spherical indenters to model individual *hpz*s are described. In these experiments, the effects of ice temperature, indenter size and structural stiffness on the failure properties have been analyzed. These tests have been carried out to study links between observed failure behavior of *hpz*s and structural response for a range of temperatures (between -1^oC and -20^oC), with areas on the order of 10^3-$10^4 mm^2$ and for structures having three different levels of stiffness (ranging from 2.67×10^7- $4.64\times10^8 N/m$). The average failure pressure was found to be negatively correlated with indenter size, as is expected due to well-known pressure-area effects in ice. The peak failure pressure was also found to be affected by ice temperature, with colder ice resulting in higher *hpz* pressures. Of particular interest is the observation that the maximum *hpz* loads were found to be insensitive to structural stiffness, while the percentage of force drop was highly dependent on structural compliance. The results have been incorporated into a statistical model of *hpz* failure, which will be integrated into ongoing development of *hpz* based dynamic ice-structure interaction models.

KEY WORDS: Ice-structure interaction; Ice-induced vibrations; Ice indentations; High pressure zones;

INTRODUCTION

When a drifting ice sheet with sufficient driving force collides with a vertical-sided offshore structure, the localized ice failure process is dominated by spalling and crushing which generates multiple regions of high pressure, termed as high pressure zones (*hpz*s). The non-uniform nature of the contact between the ice sheet and the structure can result in local pressures (e.g. pressures over a structural grillage) which are an order of magnitude higher than the global pressure (acting over the entire nominal interaction area). Medium-scale indentation tests of ice at Pond Inlet, Baffin Island and Hobson's Choice Ice Island shows that the pressure near the center of an interaction area can be significantly higher than the pressure near the edge and the failure may be associated with regular dynamic activity as was

shown in the cyclic nature of the 'sawtooth' type load-time trace reported by Frederking et al. (1990) and Kennedy et al. (1994). These observed dynamics have been linked to the development and extrusion of a crushed ice layer at the ice-structure interaction interface. Thin-sections of the crushed layer suggest that the development of this layer occurs due to a complex interplay of a number of different processes such as pressure melting, microcracking, dynamic recrystallization and sintering (Jordaan, 2001). However, the formation of the layer is highly dependent on the interaction parameters such as interaction speed, ice temperature, indentation area and structural compliance. To study the effects of interaction parameters on the dynamics of *hpz*s and the formation of the associated crushed layer, a number of small-scale indentation test programs have been carried out (Barrette et al., 2002; Wells et al., 2011; Browne et al., 2013; O'Rourke et al., 2016a; O'Rourke et al., 2016b).

During spalling, large pieces of ice near the free surface are removed by fracture, which causes a significant load drop and a reduction in the contact area (Taylor and Jordaan, 2015). The interplay between crushing and spalling is highly influenced by interaction speed, with more spalls occurring as speed increases (Wells et al., 2011). The formation of such spalls is also influenced by the location of *hpz*s since the preferential crack growth during fracture occurs towards free edges (Mackey et al., 2007) and the frequency of spalling is directly proportional to the structural compliance (Browne et al., 2013). The crushing process is also dependent on interaction parameters since temperature plays an important role in microstructural processes in the crushed layer (Barrette et al., 2002; Browne et al., 2013; Taylor et al., 2013). In their two papers, O'Rourke et al. (2016a, 2016b) argued that the periodic formation and extrusion within the crushed layer, as well as the load transmitting mechanism between multiple *hpz*s through structural feedback, could potentially generate conditions for ice-induced vibrations which would be highly dependent on the interplay between different interaction parameters.

At the same time, the well-known pressure-area relationship highlights that ice is a scale-dependent material and to extend observed behavior to full-scale interactions, the dynamic behavior of *hpz*s needs to be studied at a larger scale. The experimental program presented herein has been designed to study the dynamics of *hpz*s with larger areas, on the order of 10^3-$10^4 mm^2$, which is much larger than any previous studies and is approximately the size of individual *hpz*s during larger scale interaction (Taylor et al., 2019). In this paper, some preliminary results of the medium-scale tests are presented to investigate the sensitivity of *hpz* failure force on ice temperature and structural compliance.

EXPERIMENTAL SETUP

The results used in this analysis come from a series of medium-scale ice crushing dynamics tests performed in the Structure Laboratory of Memorial University. A confined cylindrical ice sample with a diameter of $1m$ and height of approximately $45cm$ was subjected to continuous indentation using three different sizes of indenters. The main test frame consists of a steel structure mounted on four concrete pillars which housed the indentation system shown in Figure 1. An Enerpac GPEx5 series electric pump with a reservoir capacity of 40 liters and flow rate of $2.0L/min$ (at maximum pressure) was used as the hydraulic drive system. The pump was connected to a $500ton$ Enerpac double acting cylinder with a maximum stroke of $30cm$. The maximum speed of the hydraulic system was $2.536mm/s$ and was used for all the tests considered in this analysis.

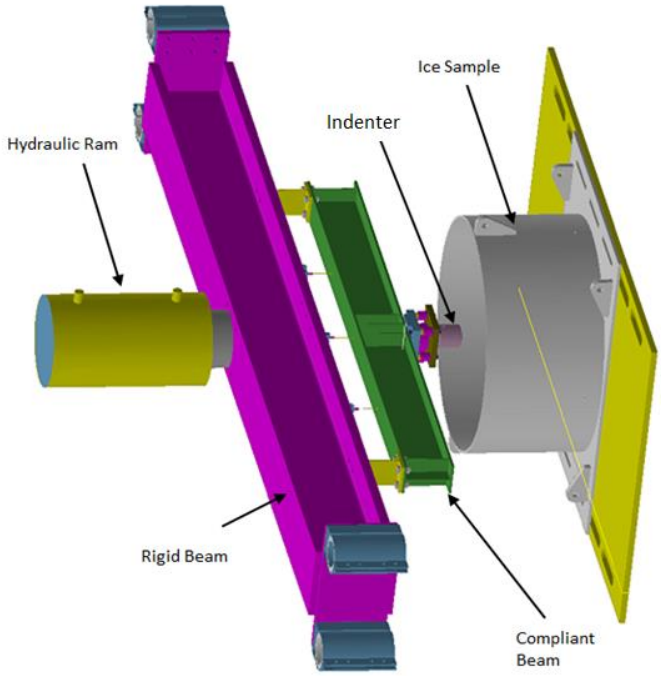

Figure 1. CAD drawing of the indentation system

A Universal Tension & Compression Shear Web Load Cell with a maximum capacity of 445kN was used to measure the ice load applied to the indenter. A linear variable displacement transducer (LVDT) with a working range of $\pm$25.4mm was used to measure the distance travelled by the indenter in the ice sample. The surface temperature of the ice was measured by a non-contact infrared digital thermometer. Two resistance temperature detectors (RTDs) were used to measure the temperature at approximately 5cm and 15cm depth in the ice sample.

Ice samples were prepared in a cylindrical steel ice holder with 1m diameter and 50cm height. Commercially available ice blocks were used to produce ice seeds using an ice crusher and sieve with grain size ranging from 2-10mm. The ice holder was then filled with ice seeds and flooded with water chilled to $0^{o}C$. The top surface of the holder was insulated with Styrofoam to ensure unidirectional ice growth. Additional information about the experimental procedures and sample preparation can be found in Birajdar et al. (2016) and Birajdar et al. (2017).

TEST MATRIX

Results from 17 different tests were used for the analysis presented in this paper where indenter size, ice temperature and beam stiffness were the variable parameters. Depending on the test, three sizes of indenters (5cm, 10cm and 15cm) and three level of structural compliance were used. Two target temperatures were set for the ice samples (-5^{o}C and -20^{o}C); however, as the tests were not performed in the cold room, the actual temperature of the sample during the tests differed slightly from the target temperature. The full test matrix is presented in Table 1.

Table 1. Test Matrix

Test ID	Indenter Diameter (cm)	Ice Temperature (^0C)	Beam Stiffness (N/m)
T1_5_16_C1	5	-16.5	C1 (2.67×10^7)
T1_5_19_C1	5	-19.5	C1 (2.67×10^7)
T1_5_7_C1	5	-7	C1 (2.67×10^7)
T1_5_4_C1	5	-4	C1 (2.67×10^7)
T1_5_15_C2	5	-15	C2 (9.61×10^7)
T1_5_7_C2	5	-7	C2 (9.61×10^7)
T1_5_16_C3	5	-16	C3 (4.64×10^8)
T1_5_7_C3	5	-7.5	C3 (4.64×10^8)
T1_10_18_C1	10	-18	C1 (2.67×10^7)
T1_10_7_C1	10	-7	C1 (2.67×10^7)
T1_10_17_C2	10	-17.5	C2 (9.61×10^7)
T1_10_6_C2	10	-6	C2 (9.61×10^7)
T1_10_15_C3	10	-15	C3 (4.64×10^8)
T1_10_6_C3	10	-6	C3 (4.64×10^8)
T1_15_18_C1	15	-18.5	C1 (2.67×10^7)
T1_15_6_C1	15	-6	C1 (2.67×10^7)
T1_15_6_C2	15	-6	C2 (9.61×10^7)

RESULTS & DISCUSSION

Definition of independent *hpz* failure

Continuous indentation was performed in each test until either the maximum load limit ($\approx$70000lb) or the maximum displacement limit of the indenter within the ice ($\approx$50mm) was reached. To identify whether the failure behavior differs significantly with the depth of indentation, Figure 2 showing the force vs. depth has been plotted. As may be observed from this figure, for test T1_5_15_C2 the peak force of *hpz* failure is found to be insensitive of indentation depth. A similar trend was observed for other tests as well and therefore, each of these load drops has been interpreted as an independent *hpz* failure event and the rest of the analysis is based on this assumption. It should be noted here that this assumption is only valid since the ratio between the indentation depth and sample diameter is very small ($\approx$ 0.05). For higher ratios between the indentation depth and sample diameter, confinement may have a significant effect on failure strength and should be addressed accordingly.

As discussed by Birajder et al. (2016), for warm ice, especially when the contact area is large, *hpz*s fails due to damage enhanced continuous extrusion. The exact point of such failure is often difficult to interpret and is excluded from the current analysis. In this paper, only test results corresponding to cases where the *hpz*s failed in brittle manner are considered. To maintain a consistent definition of *hpz* failure, events are defined as occurring when the peak of the ascending loading curve drops more than 50% within 10 subsequent data points ($\approx$

2*ms*). For example, although event A and B in Figure 2 shows a degree of load drop, such events are not considered as an *hpz* failure event.

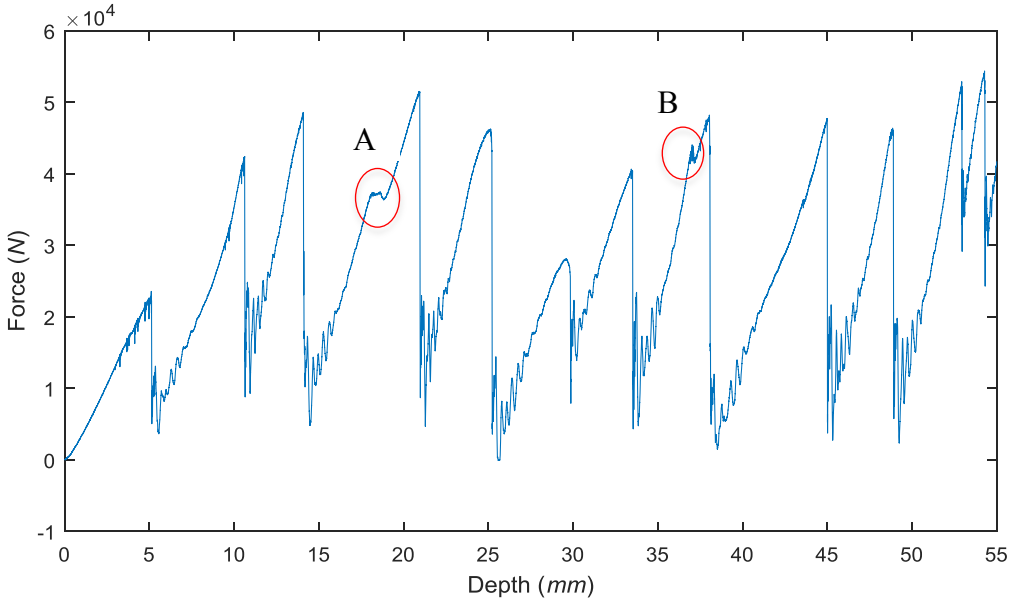

Figure 2. Force vs. Indentation Depth plot (Test ID T1_5_15_C2)

Dependence of average failure pressure on indenter size

The average or nominal failure pressure of an *hpz* was calculated by dividing the maximum force before failure with nominal interaction area. Figure 3 shows the mean value of average failure pressure plotted against indenter area with error bars of ±one standard deviation, with no corrections made for differences in temperature or beam stiffness. These results show a strong dependence of failure pressure on interaction area. Such dependence is expected, as is reflected in the "pressure-area" relationship that has been widely discussed in literature (Sanderson, 1988; Masterson et al., 2007).

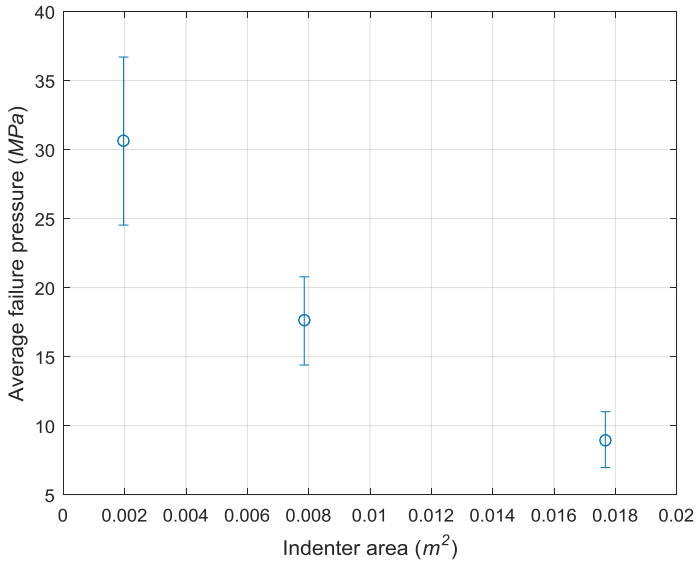

Figure 3. Mean of average failure pressure bounded by one standard deviation against indenter area

Effect of ice temperature on average failure pressure

The effect of ice temperature on failure behavior during indentation of freshwater ice has been reported previously by several authors (Browne et al., 2013; Kavanagh et al., 2015; Turner et al., 2015; Birajdar et al., 2016). As the temperature gets closer to the melting point of ice the failure behavior becomes more ductile where the peak load decreases slowly with continuous extrusion. However, in the present analysis only the 'brittle' failures of *hpz*s are being considered since no dynamic activity has been observed during events dominated by ductile ice failure. Figure 4 shows the nominal failure pressure as a function of ice temperature. To avoid the influence of scale-effects in this plot, results have been compared for a single indenter size only. Although a wide scatter is observed in the plot, the best fit line yields a negative slope suggesting that for colder ice, *hpz*s have higher average failure pressure. It is also noted that the range of scatter in the pressure data is larger for colder ice, highlighting the brittle failure behavior of cold ice. Although these results do not exhibit order-of-magnitude differences for the range of temperature considered here, such behavior can have important implication in modelling dynamic ice-structure interaction as has been explored in earlier sensitivity studies by Hossain et al. (2018).

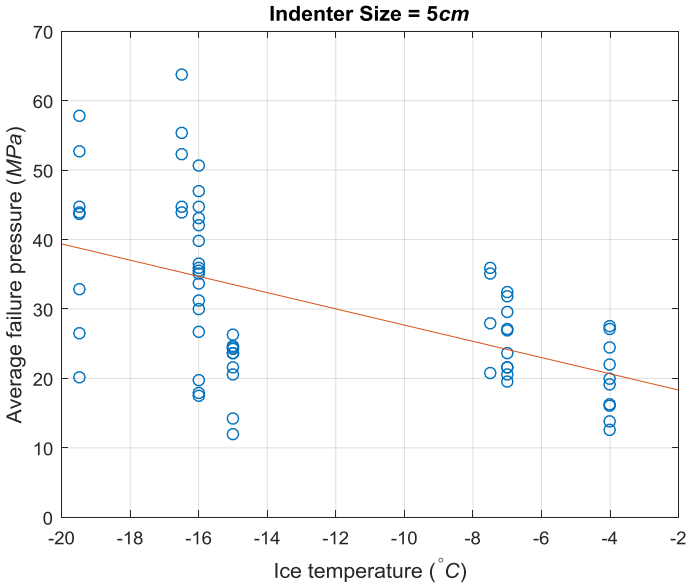

Figure 4. Average failure pressure vs. ice temperature for 5cm indenter

Effect of structural compliance on peak force and load drop

For the three level of structural compliance used for this test series, the effect of beam stiffness on failure force of *hpz* is shown in Figure 5. These results suggest that the magnitude of the failure force is independent of the beam stiffness for the test structures considered, highlighting that the peaks force during an interaction are governed by ice mechanics, not by structural parameters.

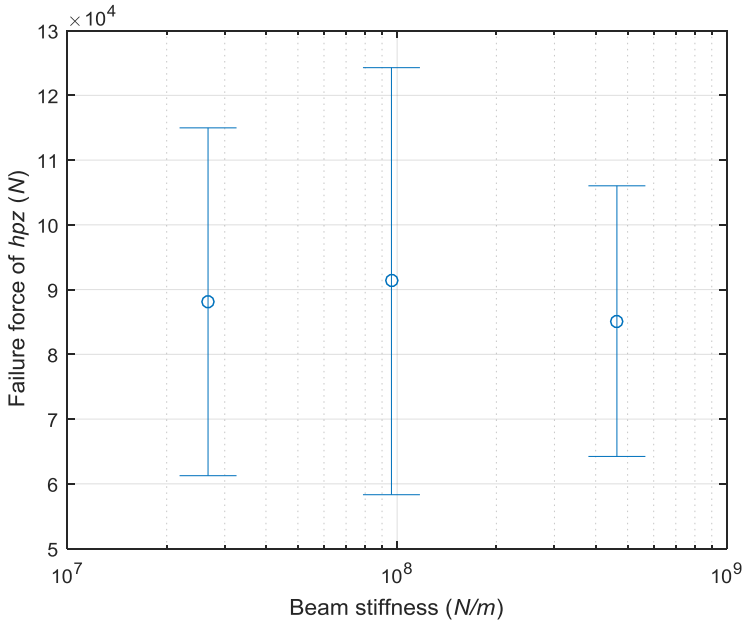

Figure 5. Failure force of *hpz* against beam stiffness

After each ice failure event, the indenter springs back due to release of stored elastic energy in the beam following a spalling event, which also results in the rapid extrusion of pulverized ice from the damaged ice layer. Although the depth of this damaged layer depends on the indenter size, ice temperature and loading rate, the extent of the extrusion process following failure was found to depend significantly on the structural compliance. Figure 6 shows the percentage of force drop for each different beam stiffness. From this plot, a clear trend may be observed. For the most compliant configuration, the mean percentage of force drop is about 95% suggesting that irrespective of the depth of the crushed layer which forms during the loading cycle, nearly all of the this damaged ice gets extruded upon failure and the next cycle of loading would therefore start with the indenter being in contact with nearly 'intact' ice. On the other hand, the stiffest configuration shows significantly less force drop after failure occurs, suggesting far less damaged ice is removed during a given load cycle and a major portion of the damaged layer survives between subsequent cycles. This observation has important implications since the transient vibration following the load drops has been linked to vibration within the crushed layer (Jordaan, 2001; O'Rourke et al., 2016a). It should be noted here that the so-called 'intact' ice still exhibits considerable microstructural damage, but the extent of the damage in the ice beneath the indenter at the end of the rebound cycle is expected to be significantly less than is present in the crushed layer beneath the indenter during the upswing phase of the loading cycle.

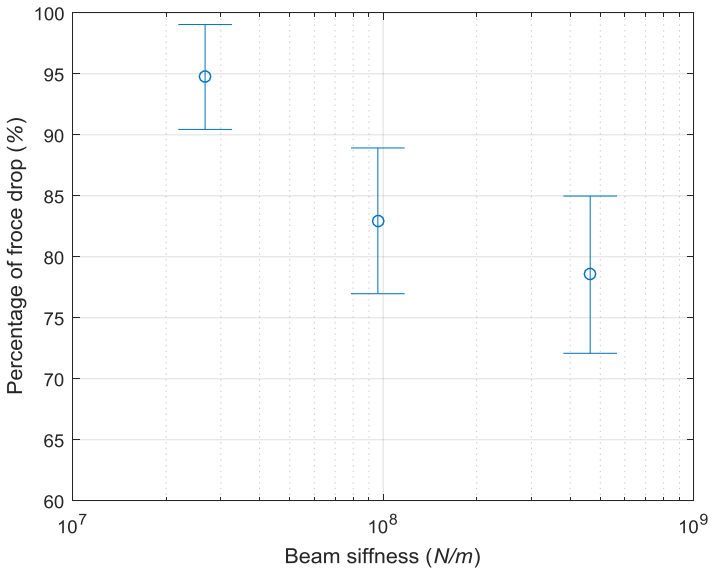

Figure 6. Percentage of force drop as a function of beam stiffness. Results showing mean with one standard deviation

CONCLUSION

In this paper *hpz* failure behavior has been characterized using results from a series of medium-scale ice crushing dynamics tests for different indenter size, ice temperature and structural stiffness. The *hpz*s studied had areas on the order of 10^3-$10^4 mm^2$, which is much larger than previous laboratory studies, and are comparable in size with *hpz*s found in other near full-scale datasets. Only brittle type failure has been considered here, where the force-time curve is 'sawtooth' in nature. Each of the load drops was considered as an independent *hpz* failure, and the well-known pressure-area effect was observed for different indenter sizes. Failure pressure was observed to exhibit some dependency on ice temperature, with colder ice having higher average failure pressures. While the different levels of structural stiffness do not seem to have a significant effect on the magnitude of the *hpz* failure force, the extent of the load drop following failure and the associated structural feedback response were found to be highly dependent on the stiffness. Structures that are more compliant were observed to produce higher load drops (thus producing greater potential feedback response). The feedback response of the structure will have a significant effect on the layer behavior since the extent of the damaged layer which survives each load cycle depends on a complex interplay between the response of the structure and the rate of damage accumulation and layer formation in the ice. This result provides valuable insight into the nature of the interplay between fracture, damage and structural response during dynamic ice-structure interactions. Work is underway to further investigate the characteristics of *hpz* failure behavior to better understand these processes and integrate these results into dynamic ice-structure interaction models.

ACKNOWLEDGEMENT

The authors gratefully acknowledge funding from Hibernia Management and Development Company, Ltd. (HMDC), Terra Nova Development (Suncor Energy Inc. - Operator), InnovateNL and the Natural Sciences and Engineering Research Council of Canada (NSERC) for this work. Use of facilities and other practical support provided by C-CORE is gratefully acknowledged.

REFERENCES

Barrette, P., Pond, J., Jordaan, I., 2002. Ice damage and layer formation in small-scale indentation experiments. Proceedings of the 16th IAHR International Symposium on Ice, Dunedin, New Zealand, December 2-6, 2002, vol.3, 246-253.

Birajdar, P.R., Taylor, R.S., Hossain, R.B., 2017. Analysis of the effect of structural compliance during medium-scale laboratory tests on ice crushing dynamics. The 27th International Ocean and Polar Engineering Conference, San Francisco, California, USA, June 25-30, 2017.

Birajdar, P., Taylor, R., Habib, K., Hossain, R., 2016. Analysis of medium-scale laboratory tests on ice crushing dynamics. Arctic Technology Conference, St. John's, NL, October 24-26, 2016.

Browne, T., Taylor, R., Jordaan, I., Gürtner, A., 2013. Small-scale ice indentation tests with variable structural compliance. Cold Reg. Sci. Technol. 88, 2-9.

Frederking, R., Jordaan, I., McCallum, J., 1990. Field tests of ice indentation at medium scale: Hobson's Choice ice island 1989. Proceedings of the 10th IAHR International Symposium on Ice, Espoo, Finland, August 20-23, 1990, vol.2, 931-944.

Hossain, R., Taylor, R., Moro, L., 2018. An assessment of sensitivity of the self-excited modelling approach for simulating dynamic ice-structure interactions to changes in temperature and scale effects. Ocean Engineering 165, 410-425.

Jordaan, I.J., 2001. Mechanics of ice-structure interaction. Eng. Fract. Mech. 68(17-18), 1923-1960.

Kavanagh, M.B., O'Rourke, B.J., Jordaan, I.J., Taylor, R.S., 2015. Observations on the Time-Dependent Fracture of Ice; International Conference on Offshore Mechanics and Arctic Engineering. Proceedings of the ASME 2015 34th International Conference on Ocean, Offshore and Arctic Engineering (OMAE2015), St. John's, Newfoundland, Canada, May 31-June 5, 2015, vol.8.

Kennedy, K.P., Jordaan, I.J., Maes, M.A., Prodanovic, A., 1994. Dynamic activity in medium-scale ice indentation tests. Cold Regions Science and Technology 22, 253-267.

Mackey, T., Wells, J., Jordaan, I., Derradji-Aouat, A., 2007. Experiments on the fracture of polycrystalline ice. Proceedings of the 19th International Conference on Port and Ocean Engineering under Arctic Conditions (POAC'07), Dalian, China, June 27-30, 2007, vol.1, 339-349.

Masterson, D., Frederking, R., Wright, B., Kärnä, T., Maddock, W., 2007. A revised ice pressure-area curve. Proceedings of the 19th International Conference on Port and Ocean Engineering under Arctic Conditions (POAC'07), Dalian, China, June 27-30, 2007, vol.1, 305-314.

O'Rourke, B.J., Jordaan, I.J., Taylor, R.S., Gürtner, A., 2016a. Experimental investigation of oscillation of loads in ice high-pressure zones, part 1: Single indentor system. Cold Reg. Sci. Technol. 124, 25-39.

O'Rourke, B.J., Jordaan, I.J., Taylor, R.S., Gürtner, A., 2016b. Experimental investigation of oscillation of loads in ice high-pressure zones, part 2: Double indentor system — Coupling and synchronization of high-pressure zones. Cold Reg. Sci. Technol. 124, 11-24.

Sanderson, T.J.O., 1988. Ice Mechanics : Risks to Offshore Structures. Graham & Trotman, London, UK ; Boston.

Taylor, R., Browne, T., Jordaan, I., Gürtner, A., 2013. Fracture and damage during dynamic interactions between ice and compliant structures at laboratory scale. Proceedings of the ASME 2013 32nd International Conference on Ocean, Offshore and Arctic Engineering (OMAE2013), Nantes, France, June 9–14, 2013, vol.6.

Taylor, R.S., Jordaan, I.J., 2015. Probabilistic fracture mechanics analysis of spalling during edge indentation in ice. Eng. Fract. Mech. 134(1), 242-266.

Taylor, R.S., Richard, M., Hossain, R., 2019. A Probabilistic High-Pressure Zone Model for Local and Global Loads During Ice-Structure Interactions. Journal of Offshore Mechanics and Arctic Engineering 141(5), 051604-051604-10.

Turner, J.D., O'Rourke, B.J., Jordaan, I.J., Taylor, R.S., 2015. Surface Temperature Fluctuations in Ice Indentation Tests; International Conference on Offshore Mechanics and Arctic Engineering. Proceedings of the ASME 2015 34th International Conference on Ocean, Offshore and Arctic Engineering (OMAE2015), St. John’s, Newfoundland, Canada, May 31-June 5, 2015, vol.8.

Wells, J., Jordaan, I., Derradji-Aouat, A., Taylor, R., 2011. Small-scale laboratory experiments on the indentation failure of polycrystalline ice in compression: Main results and pressure distribution. Cold Reg. Sci. Technol. 65(3), 314-325.